Desalination and Water Treatment
www.deswater.com

doi: 10.5004/dwt.2023.29707

300 (2023) 136–143
July

Effective removal of Congo red dye from aqueous solution using activated MgO-nanoparticles

T.E. Rasilingwani[a], J.R. Gumbo[b], V. Masindi[c,d,*], K.L. Muedi[d], R. Mbhele[e]

[a]*Department of Ecology and Resources Management, University of Venda, Private bag X5050, Thohoyandou 0950, Limpopo, South Africa, Tel.: +27 15 962 8563; email: rasilingwani.te@gmail.com*
[b]*Department of Hydrology and Water Resources, School of Environmental Sciences, University of Venda, Private bag X5050, Thohoyandou 0950, Limpopo, South Africa, Tel.: +27 15 962 8563; email: jabulani.gumbo@univen.ac.za*
[c]*Magalies Water, Scientific Services, Research & Development Division, Erf 3475, Stoffberg Street, Brits 0250, South Africa, Tel.: (012) 381-6602; email: masindivhahangwele@gmail.com*
[d]*Department of Environmental Sciences, College of Agriculture and Environmental Sciences, University of South Africa (UNISA), P.O. Box: 392, Florida 1710, South Africa, Tel.: (012) 381-6602; email: khathumuedi@gmail.com*
[e]*Council for Scientific and Industrial Research (CSIR), Smart Places, Water Centre, South Africa, email: rmbhele@csir.co.za*

Received 5 July 2022; Accepted 15 June 2023

ABSTRACT

Herein, the removal of Congo red (CR) dye from aqueous solution using MgO nanoparticles (MgO-NPs) was reported. Batch experiments were used to fulfil the objectives of this study. Specifically, the one-factor-at-a-time (OFAAT) mode where the effect of contact time, MgO-NPs dosage, and initial CR dye concentration were appraised. Results were underpinned by advanced and state-of-the-art analytical techniques. Optimum conditions were observed to be 30 mins of mixing, 1 g of MgO-NPs dosage, and 120 mg/L of initial CR concentration. X-ray fluorescence confirmed that there is no change in elemental constituents of raw and reacted materials except for the reduction of the alkaline generating fraction, that is, MgO, embedded on the nanomaterial. Furthermore, X-ray diffraction confirmed the formation of new phases after the interaction hence confirming dissolution and deposition. Fourier-transform infrared spectroscopy denoted the presence of 879 cm^{-1} band which is assigned to the asymmetric and symmetric stretching vibrations of the sulfonate ($–SO_3–$) group of CR. Microstructurally, the MgO-NPs comprised uniform flower-like microstructures with mono-dispersed and surface-wide flower-like microspheres and twisted nanosheets hence indicating deposition and dissolution of fractions from the MgO-NPs. Findings from this study will go a long way in curtailing ecological impacts posed by CR-dye in different receiving environments. Future research should look into the upscaling of this technology in industries.

Keywords: Congo red dye; Activated MgO-NPs; Wastewater treatment; Contaminants removal; Pollution control

1. Introduction

The contamination of surface water has been an issue of prime concern to environmental custodians at different spheres of management [1]. This is exasperated by notorious eco-toxicological effects posed by wastewater streams to the receiving environments. In response, regulatory bodies have developed stringent regulatory frameworks that demands the treatment of water prior discharge to the receiving environments [2]. Amongst these wastewater streams, effluents that emanates from printing industry, clothing, textile, food, and pulp industries are of major

* Corresponding author.

environmental concern and they require effective treatment. This problem is expected to grow since consumerism is drastically growing, especially in low-and-middle-income (LMI) countries [3,4]. As a counter-measure, various technologies have been developed for the removal of contaminants from aqueous solution but these technologies were documented to comprise variety of pros and cons thus fuelling the need for new and innovative technologies [5,6].

Amid the quest for pragmatic technologies for the decolouration of wastewater emanating from printing, clothing, textile and cosmetics industries [1], scientists are deeply in search for cheap, effective and efficient technologies that can be used for the removal of anionic, cationic and neutral dyes [1,5,7]. Specifically, the discharge of effluents rich in dye residues notoriously impart colour to the receiving ecosystems, hence affecting their aesthetic values. Moreover, these compounds are persistent due to their non-biodegradable nature and they are highly toxic to living organisms [1,5]. In the families of the discovered dyes, Congo red (CR) has received paramount attention primarily due to its highly toxic nature [8,9].

Based on epidemiological reports and eco-toxicity studies, exposure of living organisms to CR dye can cause variety of allergies and dermatitis along with eye, skin, and gastrointestinal irritation. Also, the exposure could lead to various mutations, vomiting, and diarrhoea in human [10–12]. Also, its unique chemical characteristics foster its metabolization to benzidine which ultimately pose variety of carcinogenic endpoints. Miandad et al. [13] further verified this finding by highlight the feasibility of CR to cause cancer and liver tumours for living organisms if ingested. Furthermore, the deposition of dye prevents penetration of sunlight to benthic sphere of an aquatic system, hence limiting the gas solubility and hindering the photosynthesis process, thus suffocating the flora and fauna components of the hydrosphere [1,14].

To date, a number of treatment technologies have been developed for the removal of dyes from aqueous solutions and they include adsorption [15], precipitation [16], photocatalysis [17], filtration [18], biosorption [19], and ion-exchange [20] processes. Depending of the scale of application, some technologies succeed and some fail, and this is attributed to the fact that CR is a very stable organic compound which is intractable with respect to chemical or biological degradation and is also very resistant to oxidizing agents, aerobic digestion, heat and light degradation [12,21]. Besides, the precipitation process has been regarded the best technology for decolouration of water [1,5]. This is motivated by the fact that other water technologies have a number of drawbacks. For example, membrane and ion exchange technologies are good but they are energy intensive, generates brine, and require regular cleaning of the membrane, that is, fouling control. Moreover, the cost associated with membrane fouling is very high, thus making the technology expensive [22]. Photocatalysis and bio-(phyto)-remediation require light and space for their effectiveness. Adsorption require regeneration and it also lose the adsorption capacity with time [1,5]. The limited capacity of adsorption to concentrated solution further demote its preference in water treatment technologies [1,23].

Various nanomaterials such as clay, metals, and their composites have been employed for the removal of dyes [24,25]. Specifically, Mg and clay-based materials have been widely applied for decolouration of water [26,27]. Xu et al. [28] evaluated the adsorptive removal of an anionic dye Congo red by flower-like hierarchical magnesium oxide (MgO)-graphene oxide composite microspheres. Ziane et al. [21] evaluated the ability of single and binary adsorption of Reactive black 5 and Congo red on modified dolomite and the results revealed that the modified dolomite. This is an indication that magnesium and calcium-based materials have been used for the removal of colour and they have massive potential. In light of that, this study seeks to explore the potential application of thermo-mechano-activated cryptocrystalline magnesite MgO nanoparticle (MgO-NPs) for the removal of CR dye from aqueous solution. Furthermore, cryptocrystalline magnesite is an endemic mineral in the northern part of South Africa and it has been widely used for the treatment of wastewater [29]. It has been used for acid mine drainage treatment [30,31], defluoridation [32], removal of oxyanions [33,34] and as a precursor for struvite synthesis [35–38]. However, activated magnesite (MgO-NPs) has never been used for the decolouration of water and this will be the first study, in design and execution, to explore this novel research avenue. Findings from this study will go a long way is demonstrating prudent and pragmatic ways to contain and manage effluents that are dye rich.

2. Materials and methods

2.1. Materials

Cryptocrystalline magnesite was collected from a derelict magnesite mine in Limpopo Province, South Africa. Dyes effluent was collected from a printing industry in Pretoria. For optimisation studies, synthetic CR dye was obtained from Merck (Germany). The used materials were of analytical grade and they were used without any further processing except for magnesite that needed some thermo-mechano-chemical activation to produce MgO-NPs. The structure of the CR dye used in this study is shown in Fig. 1.

2.2. Thermo-mechano-chemical activation of the magnesite

A vibratory ball miller was used for the processing of magnesite, that is, milling. Specifically, the samples were grinded into fine powder using Retsch RS 200 miller equipped with a vibratory ball. Thereafter, the product mineral was sieved through 32 μm perforated sieve.

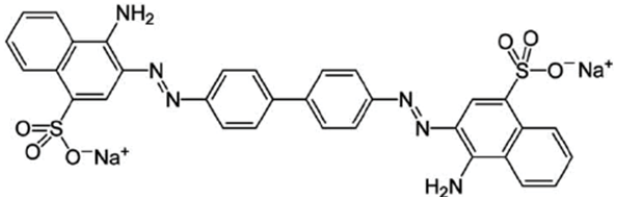

Fig. 1. Molecular structure of the Congo red dye.

The resultant powder was calcined at ≥900°C, as reported in literature [39–41]. After milling, the samples were stored in zip-lock plastic bags until utilisation for the removal of CR dye. The material will be called MgO-NPs in this study.

2.3. Preparation of CR dye stock solution

The simulated CR dye stock solution was prepared using the original sample acquired from Merck (Pty) Ltd., (South Africa). The solution was prepared into 1,000 mL volumetric flask. The mixture was thoroughly mixed and stored in a safe place until utilization for the removal experiments. Depending on the planned experiment, serial dilutions of CR dye were prepared into individual containers. The CR content was determined as described in below. The demonstration of the standard of the CR dye concentration in solution using UV-Vis spectroscopy is shown in Fig. 2.

2.4. Optimization of operational parameters

To establish conditions that are suitable for the removal of CR dye from aqueous solution using MgO-NPs, the effects of mixing time, MgO-NPs dosage, and initial concentration were evaluated. For quality control, the experiments were done in triplicate and the results were reported as mean values.

2.4.1. Effect of contact time

To determine the effect of contact time, a total of nine aliquots (100 mL) of 10 mg/L CR dye were pipetted into 250 mL containers. Thereafter, 1 g of the MgO-NPs sample was added into each container. The mixtures were then equilibrated for 1, 5, 10, 15, 20, 25, 30, 45, and 60 min at 250 rpm using the Stuart reciprocating shaker. The removal of CR dye was analysed by measuring the absorbance with a UV/Vis spectrophotometer (Shimadzu UV-2450, Albert-Hahn-Str. 6-10, Duisburg, Germany) at λ_{max} = 498 nm.

2.4.2. Effect of dosage

To determine the effect of MgO-NPs dosage, a total of seven aliquots (100 mL) of 10 mg/L CR dye were pipetted into 250 mL containers. Thereafter, varying masses (ranging from 0.1–5 g) of MgO-NPs were added into each flask. The mixtures were agitated using a shaker for an optimum time of 30 min at 250 rpm. The CR dye content was determined as described in the preceding section.

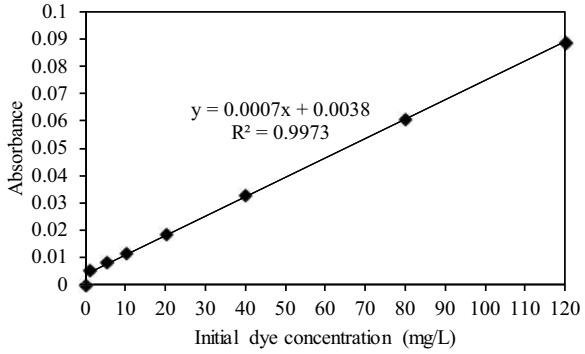

Fig. 2. Demonstration of the standard of the Congo red dye concentration in solution using UV-Vis spectroscopy.

2.4.3. Effect of concentration

To determine the efficiency of MgO-NPs on varying concentration ranges, several dilutions were made from the simulated CR stock solution. The capacity of MgO-NPs to remove CR dye from aqueous solution was then assessed at each CR dye concentration. Specified concentration that ranged between 1–120 mg/L were prepared and loaded to their respective containers. Thereafter, 1 g of MgO-NPs was added to each sample container. The mixtures were then equilibrated by shaking for 30 min using the Stuart reciprocating shaker. The CR dye content was determined as described above.

2.5. Removal of CR dye at optimized conditions

Congo red effluent emanating from a printing company in Pretoria, South Africa was treated at established optimized conditions. The primary aim was to assess the effectiveness of MgO-NPs at optimized conditions. The CR dye contents were determined as described previously. The raw and resultant solid residue were characterized, and the main quest was to gain an insight into the fates of chemical species post the interaction.

2.6. Determination of the percentage removal

The percentage removal of CR dye from aqueous solution using MgO-NPs was evaluated by the following equation.

$$\text{Percentage removal}\left(\%R\right)=\left(\frac{C_i-C_e}{C_i}\right)\times 100$$

where C_i = initial CR dye concentration (mg/L) and C_e = equilibrium CR dye concentration (mg/L).

2.7. Characterisation

To understand the fate of chemical components during the reaction of CR dye and MgO-NPs, characterisation of the feed and product solids were performed. Specifically, the morphological properties of MgO-NPs and product sludge were examined using the high-resolution (HR) – field-emission scanning electron microscope (FE-SEM) (LEO Zeiss FE-SEM, Germany) equipped with elemental dispersion spectroscopy (EDS). The functional groups of MgO-NPs and product sludge were examined using the attenuated total reflectance-Fourier-transform infrared (ATR-FTIR) spectrometer (PerkinElmer Spectrum 100 spectrometer, 710 Bridgeport Avenue Shelton, CT 06484-4794, USA), equipped with an ATR accessory and a germanium crystal. Mineralogical compositions were done using X-ray diffraction (XRD) (PANalytical X'Pert PRO-diffractometer, Enigma Business Park, Grovewood Road, Malvern WR14 1XZ, United Kingdom), analyses were performed using a Philips PW 1710 diffractometer (Kennewick, Washington,

US) equipped with graphite secondary monochromatic. Elemental composition was determined using X-ray fluorescence (XRF) (Thermo Fisher ARL-9400 XP+ Sequential XRF with Win-XRF software, Thermo Fisher Scientific, 168 Third Avenue, Waltham, MA, USA 02451). The concentration of CR dye before and after treatment was analysed by measuring the absorbance using the UV/Vis spectrophotometer (Shimadzu UV-2450) at λ_{max} = 498 nm.

3. Results and discussions

3.1. Optimisation studies

The effect of MgO-NPs on the removal of CR dye from aqueous solution under different operational parameters is summarised in Fig. 3.

As shown in Fig. 3a, the removal of CR dye was evaluated as a function of contact time. The removal efficiency was observed to increase with an increase in contact time. From 1 to 30 min, the removal efficacy increased rapidly, thereafter; there was no increase in the percentage removal of CR dye which was observed. This may be attributed to a depletion of CR dye from the aqueous system. The obtained results corresponds to the results obtained by Xu et al. [28] which reported that the removal of CR from aqueous system is very fast from 1–15 min. Hu et al. [42] reported that the use of cattail root has the ability to remove CR dye after 1 h of mixing thus demonstrating the superiority of the activated MgO-NPs over other materials reported in the literature. As such, 30 min was taken as the optimum contact time for the removal of CR dye from aqueous solution and it will be used in the subsequent experiments.

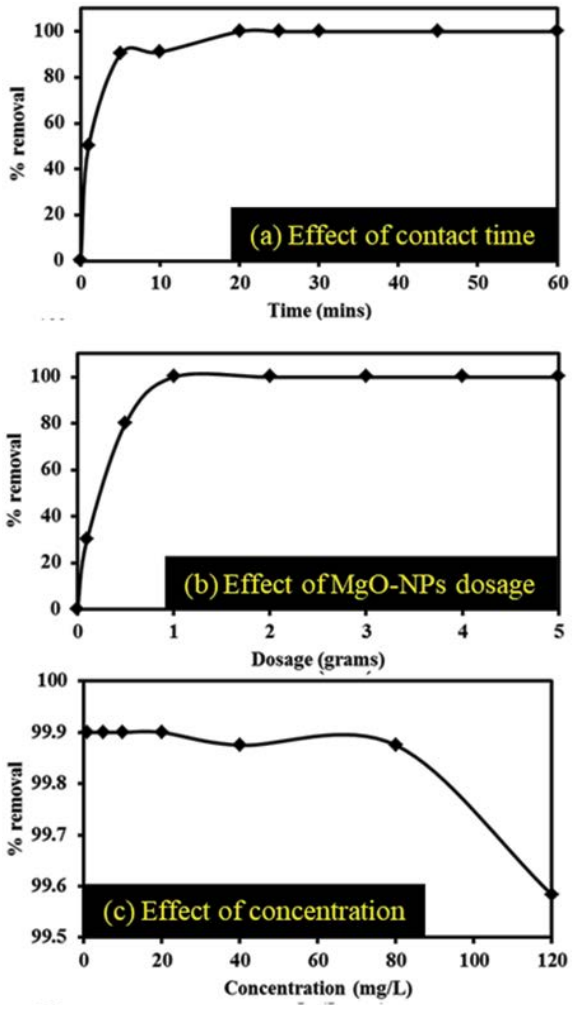

Fig. 3. Variations in the percentage removal of Congo red dye from aqueous solution using MgO-NPs. (a) Effect of contact time, (b) effect of MgO-NPs dosage, and (c) effect of concentration.

As shown in Fig. 3b, the removal of CR dye as a function of MgO-NPs dosage was evaluated and reported. As expected, there was an increase in the removal of CR dye with an increase in the MgO-NPs dosage. In particular, from 0.1 to 1 g, the CR dye removal rate was observed to increase rapidly but it was noted to have stabilised at 1 g hence denoting that there was complete depletion of CR dye from aqueous solution. The obtained results were congruent to what has been reported to literature [28,43–45]. Wang et al. [46] reported that chloride/red mud (MRM) requires 1.5 g of the feedstock dosage to effectively remove dyes from wastewater. This makes this study comparative to other materials in the same family.

Furthermore, the removal of CR dye from aqueous solution as a function of concentration was evaluated and reported (Fig. 3c). In particular, there was an increase in CR dye removal with an increase in concentration, specifically from 1 to 80, thereafter, a sharp decrease in removal efficiency was observed. This may be explained by the oversaturation of solution with an increase in CR dye concentration leading to more contaminants than the removal capacity. As such, it is clear that the concentration that is ≤120 ppm will effectively be removed from aqueous solution using 1 g of MgO-NPs. This will then be employed in the subsequent experiments.

3.2. Morphology properties

Morphology characteristics of the MgO-NPs before and after interacting with CR rich solution is shown in Fig. 4.

As shown in Fig. 4, the morphology characteristics of the MgO-NPs before (a–c) and after (b–d) interacting with CR rich solution were investigated using FE-SEM. In particular, raw MgO-NPs demonstrated the presence of uniform flower-like microstructures with an average diameter of approximately 500 nm ≤ 1 μm. These monodispersed flower-like microspheres are composed of many twisted nanosheets as the building blocks, which connect to each other. However, after contacting CR dye rich water, the resultant morphological microstructures comprised changed morphologies and the material had unseized blocks. This is a sheer indication of possible deposition of CR dye matrices onto the MgO-NPs surfaces. Moreover, change in morphological characteristics denote the alteration of chemical and mechanical properties of the material.

3.3. Mineralogical characteristics

Mineralogical characteristics of the MgO-NPs before (a–c) and after (b–d) interacting with CR rich solution is shown in Fig. 5.

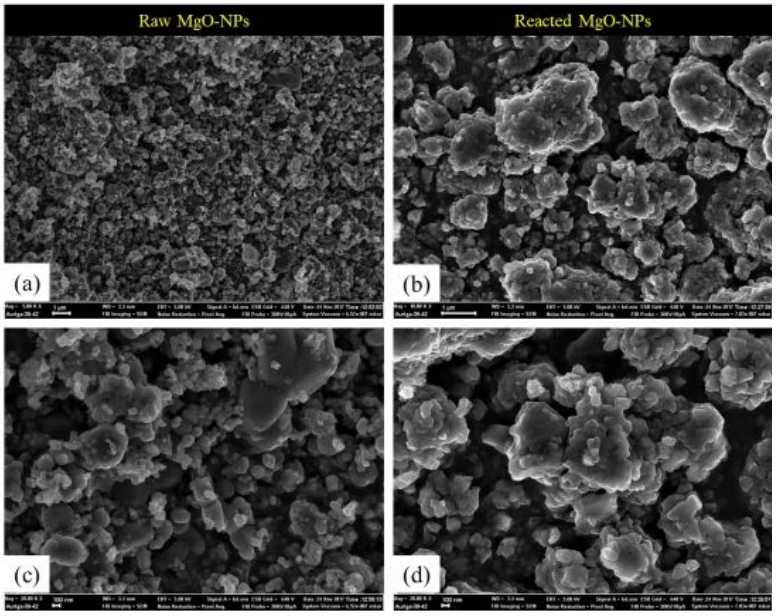

Fig. 4. Morphology characteristics of the MgO-NPs before (a–c) and after (b–d) interacting with Congo red rich solution.

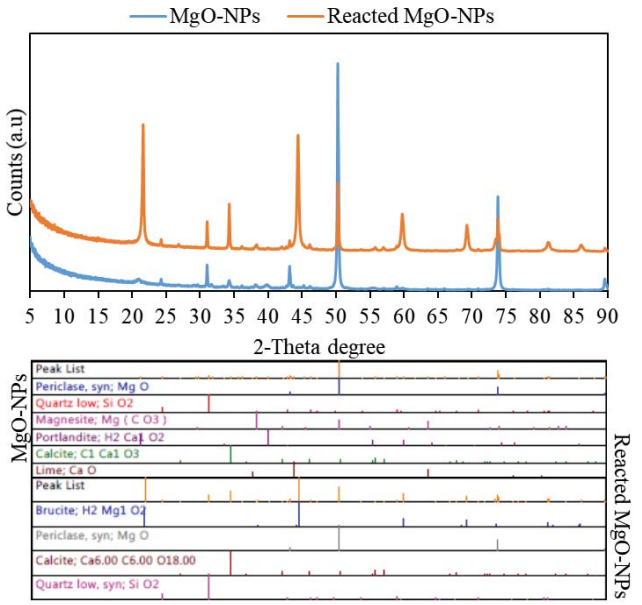

Fig. 5. Mineralogical characteristics of the MgO-NPs before and after interacting with Congo red rich solution.

As summarised in Fig. 5, crystal mineralogical compositions of MgO-NPs before and after interacting with CR rich solution are demonstrated. Specifically, the MgO-NPs comprised peaks of MgO, $MgCO_3$, SiO_2, and $CaCO_3$. However, after contacting the CR dye rich water, the mineralogical composition was observed to have changed hence denoting the formation of a new mineral phase as a result of chemical reactions. Furthermore, change in phases may be attributed to the deposition of new chemical matrices after the interaction of CR dye and MgO-NPs.

Table 1
Elemental characteristics of the MgO-NPs before and after interacting with Congo red rich solution

Element	SARM49			
	Certified	Analysed	MgO-NPs	Reacted MgO-NPs
SiO_2	99.6	99.70	4.20	3.38
TiO_2	0.01	0.00	<0.01	0.00
Al_2O_3	0.05	0.01	0.15	0.16
Fe_2O_3	0.05	0.01	0.17	0.21
MnO	0.01	0.00	0.02	0.01
MgO	0.05	0.01	82.90	62.80
CaO	0.01	0.01	5.23	5.71
Na_2O	0.05	0.02	<0.01	0.02
K_2O	0.01	0.01	<0.01	<0.01
P_2O_5	0	0.03	<0.01	<0.01
Cr_2O_3	0	0.00	<0.01	0.10
NiO	0	0.01	<0.01	0.33
ZrO_2	0	0.01	<0.01	<0.01
SO_3	0	0.00	0.20	0.09
WO_3	0	0.00	<0.01	<0.01
CuO	0	0.00	<0.01	0.04
Co_3O_4	0	0.00	<0.01	<0.01
SrO	0	0.00	0.02	0.03
LOI	0	0.10	7.08	27.10
Total	100	99.94	99.97	99.98

3.4. Elemental characteristics

Elemental characteristics of the MgO-NPs before and after interacting with CR dye rich solution is summarised in Table 1.

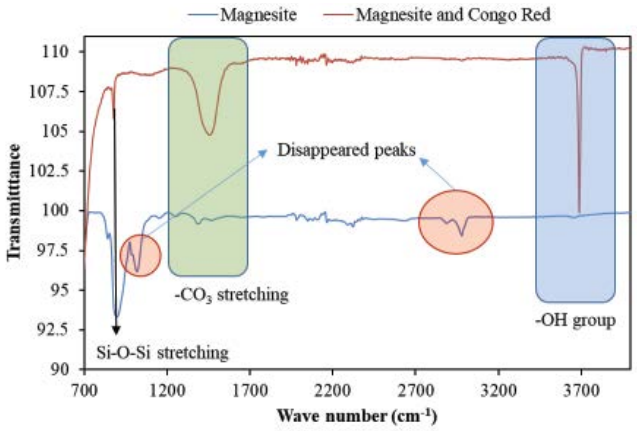

Fig. 6. Functional groups of MgO-NPs before and after interacting with Congo red dye rich solution.

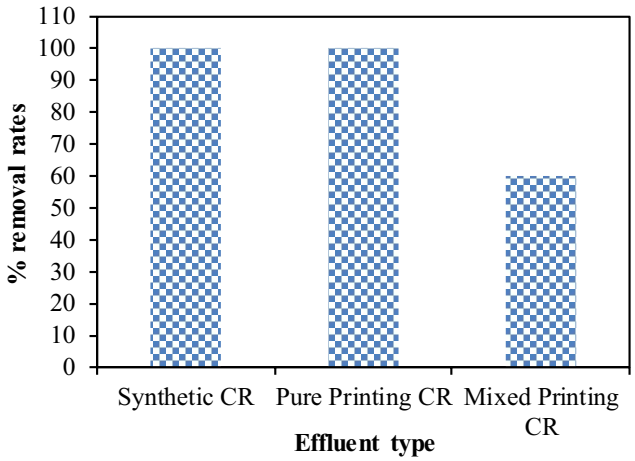

Fig. 7. The performance of MgO-NPs against aqueous matrix from different sources at optimum conditions (conditions: 30 min, 1 g/L (w/v), and 120 mg/L, at room temperature and ambient pH).

As summarised in Table 1, the elemental characteristics of MgO-NPs before and after interacting with CR rich solution was reported. From Table 1 it is clear that MgO-NPs is rich in MgO along impurities of Si and Ca. Findings from this study corroborates what has been reported in literature [29,38,41,47]. Post contacting CR rich water, the content of Mg on the matrices of MgO-NPs was observed to have decreased, however, there was an increase in the loss of ignition (LOI) hence denoting the possible formation of hydrated mineral as indicated by XRD technique.

3.5. Functional groups

Characteristics of the functional groups for MgO-NPs before and after interacting with CR rich solution is shown in Fig. 6.

The FTIR spectra of MgO-NPs before and after interacting with CR rich solution are shown in Fig. 6. Specifically, the band at 1,117 cm^{-1} correspond to symmetric stretching of carbonate, and those at 886 and 795 cm^{-1} are assigned to in-plane and out-of-plane bending vibrations of carbonate ion [48,49]. The presence of carbonates in the MgO-NPs suggests that the material was derived from magnesite with impurities of calcite [29,41]. A sharp peak at 1,039 cm^{-1} belongs to the stretching of Si–O–Si bond [50]. This also verifies the XRD results that highlighted the presence of carbonates and silicates. The weak band at approximately 1,400 cm^{-1} is associated with the stretching vibration of aromatic C=C bond [12] and this could be linked to the CR dye derivative. The band at approximately 879 cm^{-1} is assigned to the asymmetric and symmetric stretching vibrations of the sulfonate ($–SO_3–$) group of CR dye [51], confirming that CR was attached to the surface of MgO-NPs residues. The broad band at about 3,689 cm^{-1} is attributed to the stretching vibration of the –OH group [8,9] on hydrated MgO surface or in adsorbed water molecules in the interlayers of the feed material leading to the formation of hydrated minerals. The results corroborate wat has been reported by XRD technique. Based on the obtained results, MgO-NPs can act as a sink of CR dye and this could be attested by traces of building blocks of CR dye on the product sludge.

4. Treatment at optimised conditions

The performance of MgO-NPs against aqueous matrix from different sources. The treatment of these wastewater streams were undertaken at optimum conditions and the results are shown in Fig. 7.

Fig. 7 shows the efficiency of MgO-NPs on the removal of real and synthetic CR dye from aqueous matrix. In particular, MgO-NPs achieved ≥99% for synthetic and pure printing effluent whilst the mixed wastewater rich in various dyes achieved ≤60%. This could be justified by competition between contaminants in the real dye matrix from the printing industry since it is a mixture of anionic, cationic, and neutral dyes. However, findings from this study denotes the ability of MgO-NPs to remove CR dye from an aqueous system, however, its efficacy was observed to be limited aqueous matrix with cationic, anionic, and neutral dyes. This is an indication that this material can be effectively used to remove CR dye and could be up scaled to deal with the issue of CR contamination in the real operational environments. This will assist printing houses on their management of wastewater effluents.

5. Insights and mechanisms governing and underpinning CR dye removal

Various mechanisms and interplay could significantly contributes to the attenuation of CR dye from aqueous solution. Specifically, mechanisms that are governing the removal of CR dye by MgO-NPs involves the inter-actions of different facets of the CR molecule with ions embodied in MgO-NPs. In particular, when the CR dye, a typical anionic dye, is dissolved in water, the two $–SO_3$-groups give the CR molecule negative charge hence making the surface available for binding to cationic charges in the aquasphere. On the other hand, MgO-NPs has a net positive charge due to the prevalence of Mg^{2+} on its matrices. Furthermore, the protonated hydroxyl groups (i.e., $–OH^{2+}$) on the surface of the composite attract the negatively charged $–SO_3$-groups,

and this electrostatic interaction is supposedly part of the mechanisms of CR removal from aqueous media [28]. Furthermore, electrostatic attraction plays a key role in the removal of anionic dyes such as CR onto positively charged material since MgO-NPs comprise ample amount of Mg^{2+} that can form a complex with the $–SO_3$-group. This is the main mechanisms that is governing the removal of CR dye from aqueous solution. This mechanism was congruent to the results reported by FTIR and XRF, where the bond of sulfonate ($–SO_3–$) group and S oxide was observed in the resultant sludge.

6. Conclusions and recommendations

MgO-NPs were successfully employed for the removal of CR dye from aqueous solution. Optimum conditions were observed to be 30 mins of mixing, 1 g of MgO-NPs dosage (w/v), and 120 mg/L of initial CR dye concentration. XRF confirmed that there is no change in elemental constituents of raw and reacted materials except for the reduction of the alkaline generating fraction, that is, Mg, of the MgO-NPs. Furthermore, XRD confirmed the formation of new phases after the interaction hence confirming the dissolution of the material. FTIR denoted the presence of 879 cm^{-1} band which is assigned to the asymmetric and symmetric stretching vibrations of the sulfonate ($–SO_3–$) group of CR hence denoting its removal. MgO-NPs comprised uniform flower-like microstructures with monodispersed flower-like microspheres and twisted nanosheets as the building blocks connect to each other, however, the product sludge, comprised unseized blocks hence indicating deposition of fractions. Findings from this study will go a long way in curtailing ecological impacts posed by CR-dye in different receiving environments. Furthermore, future research should look into the upscaling of this novel technology.

Acknowledgements

The authors of this manuscript would like to thank the Water Research Commission (WRC), the Council for Scientific and Industrial Research (CSIR), University of South Africa, Magalies Water, and University of Venda for extending their facilities towards the accomplishment of the objectives of this project.

References

[1] T. Ngulube, J.R. Gumbo, V. Masindi, A. Maity, An update on synthetic dyes adsorption onto clay based minerals: a state-of-art review, J. Environ. Manage., 191 (2017) 35–57.
[2] Department of Water Affairs and Forestry, South African Water Quality Guidelines (First Edition), Field Guide, Department of Water Affairs and Forestry, Vol. 8, 1996.
[3] Y. Zhou, J. Lu, Y. Zhou, Y. Liu, Recent advances for dyes removal using novel adsorbents: a review, Environ. Pollut., 252 (2019) 352–365.
[4] C. Zhao, W. Chen, A review for tannery wastewater treatment: some thoughts under stricter discharge requirements, Environ. Sci. Pollut. Res., 26 (2019) 26102–26111.
[5] B. Mu, A. Wang, Adsorption of dyes onto palygorskite and its composites: a review, J. Environ. Chem. Eng., 4 (2016) 1274–1294.
[6] V. Katheresan, J. Kansedo, S.Y. Lau, Efficiency of various recent wastewater dye removal methods: a review, J. Environ. Chem. Eng., 6 (2018) 4676–4697.
[7] M. Vakili, M. Rafatullah, B. Salamatinia, A.Z. Abdullah, M.H. Ibrahim, K.B. Tan, Z. Gholami, P. Amouzgar, Application of chitosan and its derivatives as adsorbents for dye removal from water and wastewater: a review, Carbohydr. Polym., 113 (2014) 115–130.
[8] M. Hu, X. Yan, X. Hu, J. Zhang, R. Feng, M. Zhou, Ultra-high adsorption capacity of MgO/SiO_2 composites with rough surfaces for Congo red removal from water, J. Colloid Interface Sci., 510 (2018) 111–117.
[9] J. Zhang, X. Yan, M. Hu, X. Hu, M. Zhou, Adsorption of Congo red from aqueous solution using ZnO-modified SiO_2 nanospheres with rough surfaces, J. Mol. Liq., 249 (2018) 772–778.
[10] M. Toor, B. Jin, Adsorption characteristics, isotherm, kinetics, and diffusion of modified natural bentonite for removing diazo dye, Chem. Eng. J., 187 (2012) 79–88.
[11] M. Toor, B. Jin, S. Dai, V. Vimonses, Activating natural bentonite as a cost-effective adsorbent for removal of Congo red in wastewater, J. Ind. Eng. Chem., 21 (2015) 653–661.
[12] D. Sasmal, J. Maity, H. Kolya, T. Tripathy, Study of Congo red dye removal from its aqueous solution using sulfated acrylamide and N,N-dimethyl acrylamide grafted amylopectin, J. Water Process Eng., 18 (2017) 7–19.
[13] R. Miandad, R. Kumar, M.A. Barakat, C. Basheer, A.S. Aburiazaiza, A.S. Nizami, M. Rehan, Untapped conversion of plastic waste char into carbon-metal LDOs for the adsorption of Congo red, J. Colloid Interface Sci., 511 (2018) 402–410.
[14] A. Ausavasukhi, C. Kampoosaen, O. Kengnok, Adsorption characteristics of Congo red on carbonized leonardite, J. Cleaner Prod., 134 (2016) 506–514.
[15] M.A. Abdel-Khalek, M.K. Abdel Rahman, A.A. Francis, Exploring the adsorption behavior of cationic and anionic dyes on industrial waste shells of egg, J. Environ. Chem. Eng., 5 (2017) 319–327.
[16] J.P. Dhal, M. Sethi, B.G. Mishra, G. Hota, MgO nanomaterials with different morphologies and their sorption capacity for removal of toxic dyes, Mater. Lett., 141 (2015) 267–271.
[17] R. Hou, Y. Gao, H. Zhu, G. Yang, W. Liu, Y. Huo, Z. Xie, H. Li, Coupling system of Ag/BiOBr photocatalysis and direct contact membrane distillation for complete purification of N-containing dye wastewater, Chem. Eng. J., 317 (2017) 386–393.
[18] S. Zhao, Z. Wang, A loose nano-filtration membrane prepared by coating HPAN UF membrane with modified PEI for dye reuse and desalination, J. Membr. Sci., 524 (2017) 214–224.
[19] G.L. Dotto, E.C. Lima, L.A.A. Pinto, Biosorption of food dyes onto *Spirulina platensis* nanoparticles: equilibrium isotherm and thermodynamic analysis, Bioresour. Technol., 103 (2012) 123–130.
[20] M.S. Mohy Eldin, K.M. Aly, Z.A. Khan, A.E. Meky, T.S. Saleh, A.S. Elbogamy, Development of novel acid–base ions exchanger for basic dye removal: phosphoric acid doped pyrazole-g-polyglycidyl methacrylate, Desal. Water Treat., 57 (2016) 24047–24055.
[21] S. Ziane, F. Bessaha, K. Marouf-Khelifa, A. Khelifa, Single and binary adsorption of Reactive black 5 and Congo red on modified dolomite: performance and mechanism, J. Mol. Liq., 249 (2018) 1245–1253.
[22] K.B. Tan, M. Vakili, B.A. Horri, P.E. Poh, A.Z. Abdullah, B. Salamatinia, Adsorption of dyes by nanomaterials: recent developments and adsorption mechanisms, Sep. Purif. Technol., 150 (2015) 229–242.
[23] V. Masindi, S. Foteinis, P. Renforth, J. Ndiritu, J.P. Maree, M. Tekere, E. Chatzisymeon, Challenges and avenues for acid mine drainage treatment, beneficiation, and valorisation in circular economy: a review, Ecol. Eng., 183 (2022) 106740, doi: 10.1016/j.ecoleng.2022.106740.
[24] A. Naghizadeh, M. Kamranifar, A. Yari, M. Mohammadi, Equilibrium and kinetics study of reactive dyes removal from

aqueous solutions by bentonite nanoparticles, Desal. Water Treat., 97 (2017) 329–337.
[25] G. Zeydouni, M. Kianizadeh, Y. Omidi Khaniabadi, H. Nourmoradi, S. Esmaeili, M.J. Mohammadi, R. Rashidi, Eriochrme black-T removal from aqueous environment by surfactant modified clay: equilibrium, kinetic, isotherm, and thermodynamic studies, Toxicol. Rev., 38 (2019) 307–317.
[26] Y.O. Khaniabadi, H. Basiri, H. Nourmoradi, M.J. Mohammadi, A.R. Yari, S. Sadeghi, A. Amrane, Adsorption of Congo red dye from aqueous solutions by montmorillonite as a low-cost adsorbent, Int. J. Chem. Reactor Eng., 16 (2018), doi: 10.1515/ijcre-2016-0203.
[27] H. Biglari, S. RodríguezíCouto, Y.O. Khaniabadi, H. Nourmoradi, M. Khoshgoftar, A. Amrane, M. Vosoughi, S. Esmaeili, R. Heydari, M.J. Mohammadi, R. Rashidi, Cationic surfactant-modified clay as an adsorbent for the removal of synthetic dyes from aqueous solutions, Int. J. Chem. Reactor Eng., 16 (2018), doi: 10.1515/ijcre-2017-0064.
[28] J. Xu, D. Xu, B. Zhu, B. Cheng, C. Jiang, Adsorptive removal of an anionic dye Congo red by flower-like hierarchical magnesium oxide (MgO)-graphene oxide composite microspheres, Appl. Surf. Sci., 435 (2018) 1136–1142.
[29] V. Masindi, Conversion of cryptocrystalline magnesite to MgO nanosheets: insights into microstructural properties, Mater. Today Proc., 38 (2021) 1077–1087.
[30] V. Masindi, M.W. Gitari, H. Tutu, M. De Beer, Passive remediation of acid mine drainage using cryptocrystalline magnesite: a batch experimental and geochemical modelling approach, Water SA, 41 (2015) 677–682.
[31] V. Masindi, M.W. Gitari, H. Tutu, M. De Beer, N. Nekhwevha, Neutralization and Attenuation of Metal Species in Acid Mine Drainage and Mine Leachates Using Magnesite: A Batch Experimental Approach, Sui, Sun, Wang, Eds., An Interdisciplinary Response to Mine Water Challenges, China University of Mining and Technology Press, Xuzhou, 2014, pp. 640–644.
[32] V. Masindi, W.M. Gitari, T. Ngulube, Kinetics and equilibrium studies for removal of fluoride from underground water using cryptocrystalline magnesite, J. Water Reuse Desal., 5 (2015) 282–292.
[33] V. Masindi, M.W. Gitari, Removal of boron from aqueous solution using cryptocrystalline magnesite, J. Water Reuse Desal., 7 (2017) 205–213.
[34] V. Masindi, W.M. Gitari, Removal of arsenic from wastewaters by cryptocrystalline magnesite: complimenting experimental results with modelling, J. Cleaner Prod., 113 (2016) 318–324.
[35] A. Mavhungu, R. Mbaya, V. Masindi, S. Foteinis, K.L. Muedi, I. Kortidis, E. Chatzisymeon, Wastewater treatment valorisation by simultaneously removing and recovering phosphate and ammonia from municipal effluents using a mechano-thermo activated magnesite technology, J. Environ. Manage., 250 (2019) 109493, doi: 10.1016/j.jenvman.2019.109493.
[36] A. Mavhungu, V. Masindi, S. Foteinis, R. Mbaya, M. Tekere, I. Kortidis, E. Chatzisymeon, Advocating circular economy in wastewater treatment: struvite formation and drinking water reclamation from real municipal effluents, J. Environ. Chem. Eng., 8 (2020) 103957, doi: 10.1016/j.jece.2020.103957.
[37] A. Mavhungu, S. Foteinis, R. Mbaya, V. Masindi, I. Kortidis, L. Mpenyana-Monyatsi, E. Chatzisymeon, Environmental sustainability of municipal wastewater treatment through struvite precipitation: influence of operational parameters, J. Cleaner Prod., 285 (2021) 124856, doi: 10.1016/j.jclepro.2020.124856.
[38] V. Masindi, E. Fosso-Kankeu, E. Mamakoa, T.T.I. Nkambule, B.B. Mamba, M. Naushad, S. Pandey, Emerging remediation potentiality of struvite developed from municipal wastewater for the treatment of acid mine drainage, Environ. Res., 210 (2022) 112944, doi: 10.1016/j.envres.2022.112944.
[39] V.S.S. Birchal, S.D.F. Rocha, V.S.T. Ciminelli, Effect of magnesite calcination conditions on magnesia hydration, Miner. Eng., 13 (2000) 1629–1633.
[40] K. Sasaki, S. Moriyama, Effect of calcination temperature for magnesite on interaction of MgO-rich phases with boric acid, Ceram. Int., 40 (2014) 1651–1660.
[41] N. Magagane, V. Masindi, M.M. Ramakokovhu, M.B. Shongwe, K.L. Muedi, Facile thermal activation of non-reactive cryptocrystalline magnesite and its application on the treatment of acid mine drainage, J. Environ. Manage., 236 (2019) 499–509.
[42] Z. Hu, H. Chen, F. Ji, S. Yuan, Removal of Congo red from aqueous solution by cattail root, J. Hazard. Mater., 173 (2010) 292–297.
[43] Z. Zhang, L. Moghaddam, I.M. O'Hara, W.O.S. Doherty, Congo red adsorption by ball-milled sugarcane bagasse, Chem. Eng. J., 178 (2011) 122–128.
[44] G. Sriram, U.T. Uthappa, D. Losic, M. Kigga, H.-Y. Jung, M.D. Kurkuri, Mg–Al-layered double hydroxide (LDH) modified diatoms for highly efficient removal of Congo red from aqueous solution, Appl. Sci., 10 (2020) 2285, doi: 10.3390/app10072285.
[45] M. Shaban, M.R. Abukhadra, A.A.P. Khan, B.M. Jibali, Removal of Congo red, methylene blue and Cr(VI) ions from water using natural serpentine, J. Taiwan Inst. Chem. Eng., 82 (2018) 102–116.
[46] Q. Wang, Z. Luan, N. Wei, J. Li, C. Liu, The color removal of dye wastewater by magnesium chloride/red mud (MRM) from aqueous solution, J. Hazard. Mater., 170 (2009) 690–698.
[47] V. Masindi, S. Foteinis, M. Tekere, M.M. Ramakokovhu, Facile synthesis of halloysite-bentonite clay/magnesite nanocomposite and its application for the removal of chromium ions: adsorption and precipitation process, Mater. Today Proc., 38 (2021) 1088–1101.
[48] M.E. Mugwili, F.B. Waanders, V. Masindi, E. Fosso-Kankeu, Effective removal of ammonia from aqueous solution through struvite synthesis and breakpoint chlorination: insights into the synergistic effects of the hybrid system, J. Environ. Manage., 334 (2023) 117506, doi: 10.1016/j.jenvman.2023.117506.
[49] M. Mothetha, K. Kebede, V. Masindi, T.A.M. Msagati, Effective treatment of real acid mine drainage using MgO-metakaolinite nanocomposite, J. Water Process Eng., 51 (2023) 103370, doi: 10.1016/j.jwpe.2022.103370.
[50] V. Masindi, M.W. Gitari, H. Tutu, M. DeBeer, Synthesis of cryptocrystalline magnesite–bentonite clay composite and its application for neutralization and attenuation of inorganic contaminants in acidic and metalliferous mine drainage, J. Water Process Eng., 15 (2017) 2–17.
[51] N. Kataria, V.K. Garg, Removal of Congo red and Brilliant green dyes from aqueous solution using flower shaped ZnO nanoparticles, J. Environ. Chem. Eng., 5 (2017) 5420–5428.